Author Manuscript

Author Manuscript

Author Manuscript

Author Manuscript

HHS Public Access

Author manuscript

Int J Radiat Oncol Biol Phys. Author manuscript; available in PMC 2022 August 01.

Published in final edited form as:

Int J Radiat Oncol Biol Phys. 2021 August 01; 110(5): 1519–1529. doi:10.1016/j.ijrobp.2021.03.039.

Oxygen-Sensitive MRI: A Predictive Imaging Biomarker for Tumor Radiation Response?

Tatsuya J. Arai, Ph.D.[1], **Donghan M. Yang, Ph.D.**[1], **James W. Campbell III**[1], **Tsuicheng Chiu, Ph.D.**[2], **Xinyi Cheng, Ph.D.**[2], **Strahinja Stojadinovic, Ph.D.**[2], **Peter Peschke, Ph.D.**[3], **Ralph P. Mason, Ph.D.**[1]

[1]Department of Radiology, University of Texas Southwestern Medical Center, Dallas, TX, United States

[2]Department of Radiation Oncology, University of Texas Southwestern Medical Center, Dallas, TX, United States

[3]German Cancer Center, Heidelberg, Germany

Abstract

Purpose: To develop a non-invasive prognostic imaging biomarker related to hypoxia to predict stereotactic ablation radiation therapy (SAbR) tumor control.

Methods and materials: One hundred and forty-five subcutaneous syngeneic Dunning prostate R3327-AT1 rat tumors were focally irradiated once using CBCT guidance on a small animal irradiator at 225 kV. Various doses in the range 0–100 Gy were administered, while rats breathed air or oxygen and tumor control was assessed up to 200 days. Oxygen-sensitive MRI (T_1-weighted, ΔR_1, ΔR_2*) was applied to 79 of these tumors at 4.7 T to assess response to an oxygen gas breathing challenge on the day before irradiation as a probe of tumor hypoxia.

Results: Increasing radiation dose in the range 0–90 Gy enhanced tumor control of air-breathing rats with a TCD_{50} estimated at 59.6±1.5 Gy. Control was significantly improved at some doses when rats breathed oxygen during irradiation (*e.g.*, 40 Gy, $p<0.05$) and overall there was a modest left shift in the control curve: TCD_{50}(oxygen) = 53.1±3.1 Gy ($p<0.05$ *vs.* air). Oxygen-sensitive MRI showed variable response to oxygen gas breathing challenge; the magnitude of T_1-weighted signal response (%ΔSI) allowed stratification of tumors in terms of local control at 40 Gy. Tumors showing %ΔSI>0.922 with O_2-gas breathing challenge showed significantly better control at 40 Gy, when irradiated while breathing oxygen (75% *vs.* 0%, $p<0.01$). Meanwhile, increased radiation dose (50 Gy) substantially overcame the resistance with 50% control for poorly oxygenated tumors. Stratification of dose response curves based on %ΔSI>0.922 revealed different survival curves with TCD_{50}=36.2±3.2 Gy for tumors responsive to oxygen gas breathing

Corresponding author and statistical analysis: Ralph P. Mason, PhD, Department of Radiology, UT Southwestern Medical Center, 5323 Harry Hines Blvd., Dallas, TX 75390-9058, USA, Phone: +1 (214) 648-8926, Fax: +1 (214) 648-2991, Ralph.Mason@UTSouthwestern.edu.

The authors have no conflict of interest.

Publisher's Disclaimer: This is a PDF file of an unedited manuscript that has been accepted for publication. As a service to our customers we are providing this early version of the manuscript. The manuscript will undergo copyediting, typesetting, and review of the resulting proof before it is published in its final form. Please note that during the production process errors may be discovered which could affect the content, and all legal disclaimers that apply to the journal pertain.

Author Manuscript Author Manuscript Author Manuscript Author Manuscript

challenge, which was significantly less than 54.7±2.4 Gy for unresponsive tumors ($p<0.005$), irrespective of the gas inhaled during tumor irradiation.

Conclusions: Oxygen-sensitive MRI allowed stratification of tumors in terms of local control at 40 Gy, indicating a potential predictive imaging biomarker. Increasing dose to 50 Gy overcame radiation resistance attributable to hypoxia in 50% of tumors.

Introduction

It is widely recognized that hypoxia is associated with tumor radiation resistance [1–4], which is reflected in poorer outcome in clinical trials of many disease sites including prostate lung, kidney, head and neck, brain, cervix and breast cancer [5–10]. Hypoxia is expected to be particularly relevant in influencing hypofractionated radiation therapy such as SAbR/SBRT, where there is no opportunity for the reoxygenation associated with conventional courses of therapy.

Advances in image guidance and more precise treatment delivery techniques allow improved sparing of normal tissues and hence enable the application of large doses to tumors, unachievable with conventional radiation delivery techniques [11]. Consequently, SAbR is gaining popularity with highly successful clinical trials in the lung making this procedure standard of care for many patients with peripheral lung tumors [12, 13], while other disease sites including breast [14] and prostate [15, 16] are presently under clinical evaluation. Thus, there is an increasing need for a simple robust reliable method of assessing tumor hypoxia non-invasively.

Many methods have been proposed to evaluate tumor hypoxia, but to date there is no accepted non-invasive clinical procedure. Diverse imaging methods have been developed and demonstrated in pre-clinical studies to identify hypoxia based on exogenous reporter agents, *e.g.*, ^{19}F MRI [17], ^{1}H MRI [18] and ESR [19–21], or radionuclides for PET [21, 22]. Some reports have related pO_2 measurements in mouse or rat tumors to tumor growth delay following radiation [19, 20, 23, 24]. In other cases, surrogate markers of oxygenation have been related to radiation response [25–29].

Oxygen-sensitive MRI is particularly attractive since it exploits endogenous contrast with oxygen inhalation as a potential theranostic. Blood Oxygen Level Dependent (BOLD) MRI is directly sensitive to the concentration of deoxyhemoglobin (dHb) and responds to conversion to oxyhemoglobin (HbO_2). Correlations between apparent transverse relaxation rate ($R_2^* = 1/T_2^*$) or T_2^*-weighted signal were reported with pO_2 [30–32]. Furthermore, correlations between R_2^* and tumor growth delay following radiation have been demonstrated in some experimental tumor models [25, 29].

Meanwhile, Tissue Oxygen Level Dependent (TOLD), also referred to as oxygen enhanced (OE), MRI exploits the spin lattice relaxation rate ($R_1 = 1/T_1$) sensitivity of tissue water to the concentration of oxygen itself (pO_2), assessed as ΔR_1 or T_1-weighted signal response to an intervention. TOLD responses in tumors have been related to pO_2 [21, 26, 33, 34], but to date few studies have explored prognostic relevance with respect to radiation. TOLD response to an oxygen gas breathing challenge before radiation was related to a longer tumor

Author Manuscript Author Manuscript Author Manuscript Author Manuscript

growth delay following radiation when accompanied by oxygen breathing [26, 35, 36]. To further validate the relevance of TOLD MRI in terms of assessing tumor hypoxia, we evaluated application of a radiation boost, which was expected to overcome hypoxia, and thereby demonstrate the utility of oxygen-sensitive MRI to predict tumor control.

Methods and Materials

All animal experiments were approved by the xxxxxxxxxx Institutional Animal Care and Use Committee, complied with ARRIVE guidelines, and were performed in accordance with the National Institutes of Health guide for the care and use of laboratory animals (NIH Publication No. 8023, revised 1978).

Animal model:

145 adult male Copenhagen rats (Charles River, ~200 g) were implanted with syngeneic Dunning R3327-AT1 prostate tumors. The AT1 is a well characterized anaplastic tumor with a reported volume doubling time of 5.2 days [37]. Tumor tissue was originally provided by JT Isaacs of Johns Hopkins University [38] and we used early generation material from frozen stock, which was implanted into donor rats. Tissue was RAP tested and confirmed to be free of mycoplasma. Tumor tissue fragments from donor rats were implanted subcutaneously in the right thigh and allowed to grow to about 1 cm diameter. Tumor volume was measured using a caliper on the days of MRI and irradiation and twice weekly thereafter reducing to weekly for those tumors which regressed and were no longer detectable; volume was calculated as $V= (\pi/6)*a*b*c$, where a, b, c, are the three orthogonal diameters.

Magnetic Resonance Imaging:

MRI was performed on 79 rats on the day before radiation with a dose ≥ 30 Gy. Anesthetized rats (isoflurane (1.5%) in medical air (21% O_2; 1 L/min) delivered via a nose cone) were provided with a circulating warming pad to maintain body temperature at about 37 °C and placed in a Varian 4.7 T small animal horizontal bore MR scanner (Agilent, Palo Alto CA). Physiological parameters (temperature, respiration rate, and $\%O_2$ saturation (SpO_2)) were recorded using an MR-compatible monitoring and gating system (Model 1025 SA Instruments, Inc., Stony Brook, NY, USA). Rectal temperature was measured using a fiber optic probe and respiration rate and SpO_2 were monitored on the left hind leg in pulse oximeter mode. The right leg and tumor were placed in a 35 mm home-built radiofrequency transmit and receive solenoid volume coil matched and tuned to proton (^1H) resonance frequency (approximately 200 MHz). Scout images (axial, coronal, and sagittal images) were acquired using a gradient echo sequence. Imaging methods were based on a protocol in the literature [39]. Anatomical T_2-weighted images were acquired using a fast spin-echo (FSEMS) sequence in 3 min 12 sec. Quantitative R_1 (= $1/T_1$) measurements were acquired in a single slice chosen through the tumor center using a modified fast inversion-recovery (MFIR) method integrated with a slice-selective inversion pulse and a segmented turboFLASH acquisition with imaging parameters: inversion-recovery (TR = 6 s, TI = 0.01, 0.35, 1.4, 3.1, 5.5 s, TE = 20 ms) in 8 min 46 sec. R_1 measurements were obtained while the anesthetized animals (continuous 1.5% isoflurane) breathed medical air ($21\%O_2$) and at the

Author Manuscript Author Manuscript Author Manuscript Author Manuscript

end of the oxygen (100%O_2) breathing challenge. Interleaved dynamic blood oxygen level dependent (BOLD or R_2*) and tissue oxygen level dependent (TOLD or T_1-weighted) measurements were performed in the same slice as the R_1 measurements for about 15 minutes for baseline air and during an oxygen (100%O_2) breathing challenge (up to 15 minutes). BOLD acquisition used a spoiled multi-gradient-echo sequence (TR/TE = 150/5–60 ms, scan time = 41 s) and the TOLD sequence used a spoiled gradient-echo sequence (TR/TE = 30/5 ms, flip angle = 45^o, scan time = 8 s) providing 49 s temporal resolution (approximately 1 min when including systematic time lag between two sequential scans).

Radiation Treatment:

Within 24 hrs. of MRI, tumors were focally irradiated, while anesthetized rats breathed air or oxygen (with isoflurane, as for MRI) using a small animal X-ray irradiator (XRAD 225Cx, Precision X-Ray, Inc., North Branford, CT) operating at 225 kV and 13 mA, producing a dose rate of 3.3 Gy/min for a 40×40 mm^2 square collimator. Change in output for tumor specific apertures and midplane prescriptions was corrected in beam-on time calculations. A cone-beam CT (CBCT) image guidance system was used to ensure accurate localization to the tumor. Absolute dose calibration was performed in accordance with the recommendations of the AAPM TG-61 protocol [40]. Tumors were irradiated with a single dose (ranging from 0 to 100 Gy) delivered AP/PA to the gross tumor volume (GTV). Cohort sizes were based on prior literature emphasizing the need for more tumors close to the anticipated TCD_{50} [41], but also noting that only about 1/3 of the tumors would likely show a large TOLD response and be relatively radiation responsive [26]. There was no explicit power analysis *a priori*. To achieve focal irradiation the rat was shifted so that tumor centroid coincided with the beam isocenter based on CBCT, which clearly visualized tumors in the hind leg area. We used three different collimator sizes (10 mm, 15 mm and 20 mm in diameter) each time making sure that the entire tumor was included in beam's eye view. The prescribed dose was at midplane utilizing equally weighted AP/PA beams. Additionally, the PA beam was corrected for the carbon-fiber couch attenuation. Tumors on air breathing rats (Group 1) received doses of 0 (n=7), 10 (n=3), 20 (n=1), 30 (n=7), 40 (n=9), 50 (n=8), 60 (n=7), 70 (n=8), 80 (n=6), 90 Gy (n=7), and 100 Gy (n=7). Group 2 rats breathed oxygen for 10 minutes prior to irradiation and during irradiation: 10 (n=2), 20 (n=3), 30 (n=7), 40 (n=8), 50 (n=8), 60 (n=8), 70 (n=10), 80 (n=8), 90 Gy (n=11), and 100 Gy (n=10), respectively. Following irradiation, tumors were measured by calipers with an end point of progression requiring humane sacrifice, or 200 days with local control.

Data Processing and Analysis:

MRI data were processed using MATLAB (MathWorks, Natick, MA, USA). Regions of interest (ROIs) for tumor were drawn on each of three MRI images, T_1w, T_2w, and T_2*w in a single plane and the ROI for analysis was the area of overlap among these three images. For clarity we use plane to define an angle for imaging, slice as a specific thickness imaged in that plane, map as a parametric image and image as the grey scale signal intensity. BOLD and TOLD responses (%ΔSI) were calculated on a voxel-by-voxel basis in a single plane with respect to inhaling oxygen for the whole tumor ROI from dynamic BOLD and TOLD images, respectively, using the equation: $\%\Delta SI = SI(OXYGEN) - SI(AIR)/SI(AIR) \times 100$, based on the average baseline signal intensity when breathing air, and individual time

Author Manuscript Author Manuscript Author Manuscript Author Manuscript

points for oxygen. Noting the dynamic transition, mean signal response for oxygen was determined for the last 10 minutes after allowing for a 10-minute settling period. BOLD images were selected at a single echo time (TE = 5 ms) for analysis. R_2* (from BOLD measurement) maps were generated by fitting the transverse-relaxation data set (signal intensity, SI *vs.* TE) on a voxel-by-voxel in a single plane basis to a two-parameter, mono-exponential model: $SI(TE) = A \cdot \exp(-TE \cdot R_2^*)$. Quantitative ΔR_2* values were calculated as $\Delta R_2^* = [\text{mean } (R_2^*)_{OXYGEN} - \text{mean } (R_2^*)_{AIR}]$. R_1 maps were generated by fitting the inversion recovery data set (SI *vs.* TI) on a voxel-by-voxel basis to a three-parameter, mono-exponential model: $SI(TI) = A - B \cdot \exp(-TI \cdot R_1)$. ΔR_1 values were calculated as $\Delta R_1 = [\text{mean } (R_1)_{OXYGEN} - \text{mean } (R_1)_{AIR}]$. Only voxels that provided reliable fitting with a strong coefficient of determination ($R^2 \geq 0.95$) throughout the processing of the digital images from the quantitative ΔR_1 and ΔR_2* maps were used in statistical analysis. Parametric maps were generated and mean values calculated for each map at each time point.

Statistical Analysis:

Statistical analysis was performed using Statview 5.0 (SAS Institute) to determine mean values and standard deviation (SD) or standard error of the mean (SEM). Kaplan-Meier analysis with Breslow-Gehan–Wilcoxon test was used to compare tumor growth/survival post therapy for Groups 1 and 2 with respect to different doses and with respect to MRI parameters. TCD_{50} analysis used logistic regression in Origin Pro 8.5.

RESULTS

Radiation response:

As expected, higher radiation dose yielded greater tumor growth delay and increasing local control was observed for doses ≥40 Gy, when rats breathed air (Figure 1) or oxygen (Supplementary Fig. S1 and Supplementary Table S1). Overall, breathing oxygen enhanced tumor response to radiation as revealed by a modest left shift in the dose response curve and a decrease in the TCD_{50} (53.1±3.1 *vs.* 59.6±1.5 Gy, $p<0.05$; Figure 2), though enhanced local control at 200 days was only significant at 40 Gy (Figure 3A, p=0.0201). As expected, there was a considerable variability in tumor response to radiation (*e.g.*, 40 Gy; Figure 3B). Unirradiated tumors had a volume quadrupling time (VQT) of 11.7±1.9 days. Irradiated tumors, which did not show local control following 40 Gy irradiation, still exhibited significant growth delay on rats breathing air (48±7 days (8 of 9; p=0.0006), which increased significantly further for rats breathing oxygen (74±10 days (5 of 8); $p<0.0001$ *vs.* unirradiated and p=0.0176 *vs.* air). There was no significant difference between air and oxygen breathing groups at 30 Gy (p=0.7040) or 50 Gy (p=0.8697). For most of those tumors which ultimately progressed, a dip in volume followed by increase was generally seen (Figure 3B).

MRI characteristics:

To better understand the role of oxygen and hypoxia, we examined oxygen-sensitive MRI (T_1- and T_2*-weighted signal, R_1 and R_2*), as well as responses to oxygen gas breathing challenge (Figure 4). Some tumors showed significant changes in oxygen-sensitive MR parameters, while others were essentially unresponsive (Figure 4). For the group of 79

Author Manuscript Author Manuscript Author Manuscript Author Manuscript

tumors assessed by oxygen-sensitive MRI mean $R_2*_{(baseline)}$ = 52 6±1.7 s^{-1} SEM; mean $R_2*_{(oxygen)}$ = 52.3±1.9 s^{-1} (p=0.427; paired t-test) with ΔR_2* −0.35±0.42 s^{-1}. Mean BOLD %ΔSI=0.876±0.297. $T_{1(baseline)}$ = 1.92±0.24 s decreased significantly to $T_{1(}$oxygen) =1.84±0.24) (p<0.0001; paired t-test). Mean TOLD %ΔSI =1.30 ±0.244.

Tumor control related to MRI parameters:

a large BOLD response (ΔR_2* decreased by more than 0.67 s^{-1}) was associated with a significant difference in tumor control following 40 Gy irradiation for rats breathing air (p=0.0455), but not oxygen (p=0.5023) and was unsatisfactory for stratification (Supplementary Figure S2). Meanwhile, we determined that a threshold value of T_1-weighted MRI signal response ΔSI>0.922% allowed us to discriminate tumors that were resistant versus responsive to radiation. At 40 Gy, tumors exhibiting a small TOLD response showed rapid tumor progression, when rats breathed air or oxygen during irradiation, implying non-modulatable hypoxia (Figure 5A). Indeed, no rats with tumors exhibiting a small TOLD response survived beyond 80 days. Meanwhile, tumors showing a large TOLD response showed extensive local control with either gas (3/4 survived ≥200 days). For large TOLD response (ΔSI>0.922%) there was no benefit of 50 *vs.* 40 Gy (p=0.9049) (Figure 5B). For low TOLD response, 50% of rats survived at 50 Gy *vs.* none at 40 Gy.

Noting that stratification based on TOLD was similarly effective for both air- and oxygen-breathing rats (Figure 5A), we combined data to increase cohort sizes and improve statistical power (Figure 5B). For combined air plus oxygen groups, the threshold of %ΔSI>0.922 showed a significant difference in survival at 40 Gy (large *vs.* small TOLD p=0.0082). Increasing the radiation dose to 50 Gy achieved substantial control (50% of tumors) even for tumors exhibiting a small TOLD response, whether they breathed air or oxygen (Figure 5B). Indeed, T_1-weighted signal response effectively allowed discrimination of response across a range of doses (0–70 Gy) (Figure 6), yielding a significantly lower TCD_{50} for tumors responsive to the oxygen gas breathing challenge =38.2±3.2 versus 54.6±2.3 Gy for the unresponsive tumors (p<0.005). A change of R_1 (ΔR_1>3.6 s^{-1}) also allowed stratification of tumors on rats receiving 40 Gy, while breathing oxygen (p=0.02563) and this threshold was effective across a range of doses (Figure S2A).

Core physiological stability and response to oxygen breathing challenge:

Arterial oxygen saturation responded rapidly to switching gas from air to oxygen. SpO_2 with oxygen (after a 5 minute settling transition period) was significantly greater than for air. Typical baseline SpO_2 was stable with a range was 82 to 91% for individual rats (mean 86.4±4.3) increasing significantly to a range of 86 to 97%SpO_2 (mean 92.3±4.6) (generally, p<0.0001). Breathing oxygen did generally depress breathing rate slightly from a mean with air of 37.7 ±0.6 to 34.7 ±0.5 breaths per minute (bpm ±standard error of mean). Rectal temperature was stable throughout the investigation with mean temperature 35.4±2.4 °C. For individual tumors the temperature was stable within 0.5 °C with standard deviation <0.2 °C over 30 mins.

Author Manuscript Author Manuscript Author Manuscript Author Manuscript

DISCUSSION:

Increasing radiation dose enhanced growth delay and control of Dunning R3327-AT1 prostate tumors, as expected. Breathing oxygen tended to increase tumor growth delay, but there was clear variability in tumor response, and oxygen only enhanced tumor control at 40 Gy. We found that the magnitude of water proton T_1-weighted MRI signal response of tumors to a pre-irradiation oxygen gas breathing challenge allowed stratification in terms of tumor control and may serve as a predictive imaging biomarker.

In the current study, we chose the Dunning prostate R3327-AT1 tumor line since it is reported to grow consistently in rats and there is extensive prior literature showing radiation resistance. Peschke *et al.* have characterized radiation response extensively with respect to photons and heavy ions [37, 42] and it is considered to represent a very effective model of human prostate cancer. Our current results confirmed that the Dunning prostate R3327-AT1 tumor is relatively radiation resistant with a TCD_{50} (air) of 60 Gy (Figure 2). An interesting feature of the Dunning prostate R3327-AT1 tumors, which ultimately progressed following radiation, was continued increase in volume for about 10 days, followed by a dip in volume before regrowth (Figure 3B), as also reported by others [26, 35, 42]. This may represent radiation induced swelling or continued growth until the radiation damage causes cell death and regression prior to further regrowth. It was previously reported that breathing oxygen, enhanced radiation response of some Dunning prostate R3327-AT1 tumors coinciding with higher pO_2 as determined using ^{19}F MRI of exogenous administered hexafluorobenzene reporter molecule [43]. A further report found that tumors exhibiting a larger TOLD response to an oxygen breathing challenge before radiation experienced a longer tumor growth delay following 30 Gy radiation when accompanied by oxygen breathing [26].

At 40 Gy, addition of oxygen gave a significant benefit in terms of tumor control (survival to at least 200 days; Figure 3B), and even those tumors that were not controlled showed significantly greater tumor growth delay. However, about 60% of tumors continued to grow reaching four times their treatment volume within 200 days. Since tumor control is the ultimate goal, we sought to differentiate those tumors that were controlled from those which progressed. The TOLD measurements of response to a pre-irradiation gas breathing challenge allowed stratification in terms of tumor control. Specifically, those tumors exhibiting a small TOLD response showed much poorer control than those with large TOLD response (Figure 5A) whether rats breathed air or oxygen during irradiation. A small TOLD response corresponded with substantial radiation resistance across a range of doses yielding a higher TCD_{50} (Figure 6).

Overcoming radiation resistance:

Those tumors showing a small TOLD response (predicted to be hypoxic [26]) showed little benefit from oxygen gas breathing during irradiation. Indeed, hypoxic tumors were resistant whether rats breathed air or oxygen during irradiation, while better oxygenated tumors showed similarly good control with air or oxygen (Figure 5A). Meanwhile, applying a 10 Gy radiation boost (50 Gy *vs.* 40 Gy) showed substantial additional local control of hypoxic tumors, approaching the well-oxygenated tumors (Figure 5B). The higher dose gave no benefit to well oxygenated tumors. These results coincide with a recent study based on ESR,

Author Manuscript Author Manuscript Author Manuscript Author Manuscript

which reported that a regionally selective radiation boost (13 Gy) enhanced tumor control when applied to hypoxic regions, but not oxic regions of subcutaneous FSa fibrosarcoma tumors in mice [19]. A radiation boost has been found to enhance therapeutic cure rates for clinical prostate cancer, but higher dose inevitably increases the risk of side effects since the prostate is surrounded by sensitive tissues such as bladder, rectum and nerves [44]. Thus, the ability to identify hypoxic tumors is vital to avoid unnecessary radiation damage. Historically, carbogen ($95\%O_2+5\%CO_2$) was favored over oxygen to improve tumor oxygenation and indeed, it has been used successfully in many pre-clinical animal investigations [3, 25, 29, 32, 45] and human clinical trials (*e.g.*, ARCON) [9]. However, in the Dunning prostate R3327-AT1, carbogen was reported to show no benefit over oxygen [26]; meanwhile there are many reports that adding CO_2 causes severe respiratory distress and is unpopular with patients [1]. An alternative approach to overcoming hypoxia is use of high LET radiation such as carbon beams, which were demonstrated to be effective on the Dunning prostate tumors described here [42]. However, high LET facilities remain esoteric and thus it would be particularly important to identify those patients who would benefit.

The utility of oxygen-sensitive MRI to stratify tumors:

Oxygen-sensitive MRI based on tissue water is attractive since it is non-invasive and avoids the need for exogenous reporter molecules. R_1 is directly related to pO_2 and correlations have been shown in tumors [26, 29, 33, 34], although the direct relationship can be influenced by metal ions, deoxyhemoglobin concentration, and temperature. R_1 measurements typically require long acquisition times and therefore we only examined quantitative R_1 once at baseline and once with oxygen breathing to assess change (ΔR_1). We observed better local control for tumors exhibiting a larger ΔR_1 when irradiated while breathing air or oxygen (Supplementary Figure S2A). Indeed, in the range 40–60 Gy applying a threshold of $\Delta R_1 > 3.6\ s^{-1}$ yielded a significant difference in local control ($p=0.0223$).

T_1-weighted images provide much faster temporal resolution allowing dynamic changes to be observed directly (Figure 4). Observing a change in signal coinciding with the gas challenge adds confidence that it truly reflects a change in tumor oxygenation and any drift due to temperature would be readily apparent, although temperature was found to be stable throughout the interventions. It was previously reported that a change in T_1-weighted signal >1.6% allowed discrimination of tumors which responded to an oxygen gas breathing challenge and were therefore well perfused and better oxygenated [26]. Here, we found a slightly lower threshold was effective ($\Delta SI > 0.922\%$), but the difference is small and likely reflects the responses of the cohorts of tumors observed in the respective study populations. Indeed, a threshold on 0.922% or 1.6% gave identical Kaplan Meier survival curves here.

Cao-Pham *et al.* also examined relationships between tumor relaxation properties and radiation response, notably R_2^* and R_1 of both tissue water and lipid at 11.7 T [29]. In principle, the lipid relaxation response to changes in pO_2 could be much more sensitive, but the lipid signal intensity is much weaker. They observed reduced TCD_{50} accompanying oxygen gas breathing during irradiation, as we report here, but they reported a lack of correlation between R_1 and radiation response. It is important to note that we find the

Author Manuscript Author Manuscript Author Manuscript Author Manuscript

change in R_1 (ΔR_1) or T_1w-signal (%ΔSI) to have predictive value, not the absolute R_1. We believe that lack of R_1 response to the oxygen breathing coincides with poor perfusion, lack of change in oxygenation and extensive hypoxia. Indeed, change in R_1 has been related to tumor growth delay in pre-clinical studies of both subcutaneous prostate and orthotopic brain tumors [26, 36].

R_2* is directly influenced by the concentration of deoxyhemoglobin as the basis of BOLD MRI. Several studies have shown correlations between R_2* and tumor oxygenation [30–32] and R_2* response to a gas breathing challenge has been related to tumor growth delay in response to radiation in some tumor types, but not others [25, 26, 29]. In the current work, BOLD R_2* response provided weaker stratification than TOLD (compare Figures 6 and Supplementary Figure S2B). Baseline tumor R_2* was stable (Figure 4C), as also observed for arterial oxygenation (SpO_2) based on pulse oximetry (Supplementary Figure S3). SpO_2 responded rapidly to the oxygen gas breathing challenge, as also seen in some tumors (Figure 4C).

Quantitative R_1 and R_2* measurements are potentially more reproducible and effective than relaxation-weighted measurements and moreover R_2* can be determined essentially as rapidly as single echo time (T_2*-weighted) measurements. We acquired the full echo train, but noted that motion and noise can lead to degraded signal and we applied a filter to ensure monotonic decay of signal in individual voxels and discarded any data where fewer than five echoes were usable. R_2* primarily reflects vascular oxygenation, but is sensitive to additional tissue and physical properties, notably hematocrit, flow and vascular volume. Nonetheless, a change in R_2* accompanying a gas breathing challenge is expected to reflect conversion of deoxy- to oxy-hemoglobin and improved tumor oxygenation. Indeed, we found that a decrease in R_2*> 0.67 s^{-1} in response to oxygen challenge was associated with better control for tumors on rats breathing air during Irradiation, though not for those breathing oxygen. This threshold provided some discrimination based on TCD_{50} curves (Supplementary Figure S2B)

The current oxygen-sensitive MRI measurements are entirely non-invasive, while the traditional use of exogenous reporters has often required invasive intra tumoral injection or has potentially biased measurements towards well-perfused regions following systemic administration. Interrogating tissue water allows a whole tumor to be observed, though we selected a single central slice to avoid excessive data acquisition times. There may be concern that signal from necrotic regions would compromise predictive utility of measurements. Dynamic contrast enhanced MRI can be used to discriminate perfused versus non-perfused (presumably necrotic) regions and when combined with TOLD was found to provide better correlations with hypoxia based on pimonidazole uptake in some tumor types [46]. Combining DCE and OE-MRI adds to the complexity of the investigation requiring IV infusion of contrast agent in addition to gas breathing challenge. Combination of BOLD and TOLD is particularly simple since the respective pulse sequences are easily interleaved during a gas challenge. BOLD response is often greater than TOLD helping to identify the TOLD response and more importantly validating the observations when the responses are consistent [39].

Author Manuscript Author Manuscript Author Manuscript Author Manuscript

R_1 and R_2* measurements are readily implemented in patients and have been individually reported for various disease sites including prostate with respect to hypoxia [47, 48], but not specifically radiation responsiveness. MRI is becoming increasingly relevant to treatment planning for prostate cancer and the current studies could be important in exploiting MR-Linac treatment opportunities. For some disease sites such as prostate, the enhanced soft tissue delineation offered by MRI over CT is vital for defining tumor. This is widely applicable to patients and increasingly reported for pre-clinical small animal investigations [49]. Here, we used subcutaneous tumors for ease of implantation and irradiation, as is common in most current research. We applied uniform treatment across the whole tumor, but identification of local hypoxia might allow a specific radiation boost to hypoxic regions only. In terms of clinical relevance, the current work was performed at 4.7 T, which is a little higher than standard 3 T for patients. It should be noted that R_1 response to pO_2 tends to decrease at higher magnet field, but of course, signal to noise increases. Nonetheless, oxygen-sensitive MRI including T_1-sensitive measurements were recently reported in the tumors of human prostate cancer patients [48].

It must be noted that MRI is labor intensive and we lacked resources to perform MRI on every tumor. We first wanted to establish whether the tumors would exhibit a similar radiation response to that published [42] and assess whether there was a large oxygen gas breathing effect. As such, MRI was performed on about half the tumors, but we note other studies have similarly published results where MRI was only performed on a sub-cohort [27]). Ultimately, the addition of an MRI scan to a study is time consuming and costly, but adding oxygen-sensitive MRI to an existing scan adds little overhead. We believe the current results now provide strong impetus to further explore the predictive value of TOLD with respect to radiation therapy. Moreover, the increasing use of MRI in treatment planning for prostate cancer and recent results of the FLAME trial [50] suggest an opportunity to facilitate such measurements in human patients.

Context among imaging methods:

Many diverse imaging technologies based on exogenous reporters have been demonstrated to assess pO_2 in tumors (*e.g.*, MRI, ESR and optical [19, 43, 51]), while others reveal hypoxia (primarily bioreductive nitroimidazoles based on ^{18}F PET [52, 53]) and it is important to place the current work in context [1, 3, 17]. Investigations have explored the predictive value of oxygen-sensitive measurements before initiating radiation, as well as the separate topic of variation in hypoxia following radiation, which is particularly important to the timing of sequential doses for a typical multi fraction regimen. PET based on fluoromisonidazole (FMISO) has been particularly popular in clinical trials for several years. Rischin *et al.* showed that chemoradiation was less successful in head and neck cancer patients determined to have hypoxic tumors based on FMISO accumulation [54]. They also reported that the addition of the hypoxic-cell-selective cytotoxin tirapazamine reduced loco-regional treatment failures for patients with hypoxic tumors. Meanwhile, Lee *et al.* reported that dose de-escalation could be applied successfully to head and neck patients exhibiting minimal hypoxia at baseline, or as determined halfway through a course of treatment [55]. Kelada examined lung cancer patients at baseline, 2 and 24 hours after irradiation and noted general hypoxiation after 24 hours, which would have implications for optimal timing of

Author Manuscript Author Manuscript Author Manuscript Author Manuscript

subsequent doses. Despite promising results in patients, there remains an active pursuit of an optimal PET reporter, since FMISO provides relatively poor contrast and extensive background signal. Compared with PET, oxygen-sensitive MRI is attractive since it avoids the need for an exogenous contrast agent and the associated radioactivity. It is particularly difficult to assess dynamic changes in oxygenation using PET, since initial doses must clear or decay before additional measurements can be performed. Interestingly, correlations have been reported between TOLD and FMISO uptake, but with the caveat that PET should be performed at both early and late time points (10 minutes and 2 hours) to differentiate lack of access/perfusion versus well oxygenated tumor regions [56]. TOLD has also been reported with respect to a split dose paradigm with a change in ΔR_1 prior to the second dose, but not first dose, showing some correlation with tumor growth delay [35]. Meanwhile, the strongest correlation was observed between tumor growth delay and change in oxygen gas breathing response ($\Delta\Delta R_1$) between baseline and second doses.

Future Directions:

We have achieved statistical significance and demonstrated the ability to discriminate responsive versus unresponsive tumors, but the study would benefit from additional tumors and radiation doses, notably at 35 Gy for high TOLD and 45 Gy for low TOLD to better define the dose response curves and precision of the TCD_{50} estimates. In this study, we were able to effectively stratify tumors based on mean oxygen-sensitive MRI response from a single slice through the tumor center. In the future, it may be valuable to explore heterogeneity further across multiple slices or 3D volumes and in terms of enhancing volume fractions. We examined a single high dose of radiation, essentially radiation surgery, whereas clinical practice typically uses 3 to 5 doses fractionated over 2 weeks, and it will be important to investigate whether oxygen-sensitive MRI provides similar ability to stratify under those conditions. A report from White *et al.* [35] showed that for a split dose irradiation regimen of this same tumor type, it was the TOLD responses prior to a second radiation dose that was correlated with outcome, though actually it was the change in responses that was most predictive. It will also be important to validate these observations in additional tumor types, *e.g.*, other sublines of the Dunning prostate R3327 tumors noted for differential hypoxia and growth rates, as shown by Glowa *et al.* [42]), as well as other tumor types and ultimately orthotopic and spontaneous tumors.

Conclusions

It has been noted that “The ideal method for measuring hypoxia would be (i) noninvasive, (ii) amenable to repeated measures, (iii) high spatial resolution, (iv) cost-effective, and (v) directly translatable to human trials” [57]. The TOLD approach described here, for identifying responsive versus less responsive tumors to radiation, satisfies these criteria, although it must be noted that it provides a surrogate predictive marker related to hypoxia rather than pO_2 or hypoxic fraction directly. As SBRT becomes increasingly popular, there is a developing need to predict response, in particular the potential need for a radiation boost to overcome hypoxia associated resistance. Oxygen-sensitive MRI is practical in patients and has been demonstrated in prostate cancer. The current results indicate the potential

Author Manuscript Author Manuscript Author Manuscript Author Manuscript

predictive value as a basis for further validation in pre-clinical animal models and human clinical trials.

Supplementary Material

Refer to Web version on PubMed Central for supplementary material.

Acknowledgment:

Erica A. Mason assisted with graphics.

Funding: This work was supported in part by Cancer Prevention and Research Initiative of Texas (CPRIT) RP140285. MRI infrastructure was supported by NIH P41 EB015908, 1P30 CA142543, and an ARRA supplement to 1U24 CA126608 and irradiation was facilitated by Shared Instrumentation Grant S10 RR028011. Funders had no influence over generation of data or presentation of manuscript.

REFERENCES

[1]. Tatum JL, Kelloff GJ, Gillies RJ, Arbeit JM, Brown JM, Chao KS, Chapman JD, Eckelman WC, Fyles AW, Giaccia AJ, Hill RP, Koch CJ, Krishna MC, Krohn KA, Lewis JS, Mason RP, Melillo G, Padhani AR, Powis G, Rajendran JG, Reba R, Robinson SP, Semenza GL, Swartz HM, Vaupel P, Yang D, Croft B, Hoffman J, Liu G, Stone H, Sullivan D, Hypoxia: importance in tumor biology, noninvasive measurement by imaging, and value of its measurement in the management of cancer therapy, Int J Radiat Biol, 82 (2006) 699–757. [PubMed: 17118889]

[2]. Overgaard J, Hypoxic radiosensitization: adored and ignored, J Clin Oncol, 25 (2007) 4066–4074. [PubMed: 17827455]

[3]. Gallez B, Neveu MA, Danhier P, Jordan BF, Manipulation of tumor oxygenation and radiosensitivity through modification of cell respiration. A critical review of approaches and imaging biomarkers for therapeutic guidance, Biochim Biophys Acta Bioenerg, 1858 (2017) 700–711. [PubMed: 28088332]

[4]. Nahum AE, Movsas B, Horwitz EM, Stobbe CC, Chapman JD, Incorporating clinical measurements of hypoxia into tumor local control modeling of prostate cancer: Implications for the alpha/beta ratio, International Journal of Radiation Oncology Biology Physics, 57 (2003) 391–401.

[5]. Vergis R, Corbishley CM, Norman AR, Bartlett J, Jhavar S, Borre M, Heeboll S, Horwich A, Huddart R, Khoo V, Eeles R, Cooper C, Sydes M, Dearnaley D, Parker C, Intrinsic markers of tumour hypoxia and angiogenesis in localised prostate cancer and outcome of radical treatment: a retrospective analysis of two randomised radiotherapy trials and one surgical cohort study, Lancet Oncol, 9 (2008) 342–351. [PubMed: 18343725]

[6]. Milosevic M, Warde P, Menard C, Chung P, Toi A, Ishkanian A, McLean M, Pintilie M, Sykes J, Gospodarowicz M, Catton C, Hill RP, Bristow R, Tumor Hypoxia Predicts Biochemical Failure following Radiotherapy for Clinically Localized Prostate Cancer, Clinical Cancer Research, 18 (2012) 2108–2114. [PubMed: 22465832]

[7]. Turaka A, Buyyounouski MK, Hanlon AL, Horwitz EM, Greenberg RE, Movsas B, Hypoxic Prostate/Muscle PO_2 Ratio Predicts for Outcome in Patients With Localized Prostate Cancer: Long-Term Results, International Journal of Radiation Oncology Biology Physics, 82 (2012) E433–E439.

[8]. Hugonnet F, Fournier L, Medioni J, Smadja C, Hindie E, Huchet V, Itti E, Cuenod CA, Chatellier G, Oudard S, Faraggi M, Hypoxia G in Renal Cancer Multicenter, Metastatic renal cell carcinoma: relationship between initial metastasis hypoxia, change after 1 month's sunitinib, and therapeutic response: an 18F-fluoromisonidazole PET/CT study, J Nucl Med, 52 (2011) 1048–1055. [PubMed: 21680694]

[9]. Kaanders JH, Pop LA, Marres HA, Bruaset I, van den Hoogen FJ, Merkx MA, van der Kogel AJ, ARCON: experience in 215 patients with advanced head-and-neck cancer, Int J Radiat Oncol Biol Phys, 52 (2002) 769–778. [PubMed: 11849800]

Author Manuscript Author Manuscript Author Manuscript Author Manuscript

[10]. Fennell JT, Wiedenmann N, Oehlke O, Kraft JS, Grosu A-L, Hypoxia and positron emission tomography in patients with gliomas, Clinical and Translational Imaging, 5 (2017) 447–453.

[11]. Brown JM, Carlson DJ, Brenner DJ, The Tumor Radiobiology of SRS and SBRT: Are More Than the 5 Rs Involved?, International Journal of Radiation Oncology*Biology*Physics, 88 (2014) 254–262.

[12]. Timmerman R, Paulus R, Galvin J, Michalski J, Straube W, Bradley J, Fakiris A, Bezjak A, Videtic G, Johnstone D, Fowler J, Gore E, Choy H, Stereotactic body radiation therapy for inoperable early stage lung cancer, JAMA, 303 (2010) 1070–1076. [PubMed: 20233825]

[13]. Lester-Coll NH, Sher DJ, Cost-Effectiveness of Stereotactic Radiosurgery and Stereotactic Body Radiation Therapy: a Critical Review, Curr Oncol Rep, 19 (2017) 41. [PubMed: 28421482]

[14]. Vasmel JE, Charaghvandi RK, Houweling AC, Philippens MEP, van Asselen B, Vreuls CPH, van Diest PJ, van Leeuwen AMG, van Gorp J, Witkamp AJ, Koelemij R, Doeksen A, Sier MF, van Dalen T, van der Wall E, van Dam I, Veldhuis WB, Kirby AM, Verkooijen HM, van den Bongard H, Tumor Response After Neoadjuvant Magnetic Resonance Guided Single Ablative Dose Partial Breast Irradiation, International Journal of Radiation Oncology Biology Physics, 106 (2020) 821–829.

[15]. Alongi F, Rigo M, Figlia V, Cuccia F, Giaj-Levra N, Nicosia L, Ricchetti F, Sicignano G, De Simone A, Naccarato S, Ruggieri R, Mazzola R, 1.5 T MR-guided and daily adapted SBRT for prostate cancer: feasibility, preliminary clinical tolerability, quality of life and patient-reported outcomes during treatment, Radiation Oncology, 15 (2020).

[16]. Jackson WC, Silva J, Hartman HE, Dess RT, Kishan AU, Beeler WH, Gharzai LA, Jaworski EM, Mehra R, Hearn JWD, Morgan TM, Salami SS, Cooperberg MR, Mahal BA, Soni PD, Kaffenberger S, Nguyen PL, Desai N, Feng FY, Zumsteg ZS, Spratt DE, Stereotactic Body Radiation Therapy for Localized Prostate Cancer: A Systematic Review and Meta-Analysis of Over 6,000 Patients Treated On Prospective Studies, International Journal of Radiation Oncology*Biology*Physics, 104 (2019) 778–789.

[17]. Mason RP, Zhao D, Pacheco-Torres J, Cui W, Kodibagkar VD, Gulaka PK, Hao G, Thorpe P, Hahn EW, Peschke P, Multimodality imaging of hypoxia in preclinical settings, Q J Nucl Med Mol Imaging, 54 (2010) 259–280. [PubMed: 20639813]

[18]. Kodibagkar VD, Wang X, Pacheco-Torres J, Gulaka P, Mason RP, Proton imaging of siloxanes to map tissue oxygenation levels (PISTOL): a tool for quantitative tissue oximetry, NMR Biomed, 21 (2008) 899–907. [PubMed: 18574806]

[19]. Epel B, Maggio MC, Barth ED, Miller RC, Pelizzari CA, Krzykawska-Serda M, Sundramoorthy SV, Aydogan B, Weichselbaum RR, Tormyshev VM, Halpern HJ, Oxygen-Guided Radiation Therapy, International Journal of Radiation Oncology*Biology*Physics, 103 (2019) 977–984.

[20]. Matsumoto S, Kishimoto S, Saito K, Takakusagi Y, Munasinghe JP, Devasahayam N, Hart CP, Gillies RJ, Mitchell JB, Krishna MC, Metabolic and Physiologic Imaging Biomarkers of the Tumor Microenvironment Predict Treatment Outcome with Radiation or a Hypoxia-Activated Prodrug in Mice, Cancer Res, 78 (2018) 3783–3792. [PubMed: 29792309]

[21]. Colliez F, Gallez B, Jordan BF, Assessing Tumor Oxygenation for Predicting Outcome in Radiation Oncology: A Review of Studies Correlating Tumor Hypoxic Status and Outcome in the Preclinical and Clinical Settings, Front Oncol, 7 (2017) 10. [PubMed: 28180110]

[22]. Peeters S, Zegers CML, Lieuwes NG, van Elmpt W, Eriksson J, van Dongen G, Dubois L, Lambin P, A Comparative Study of the Hypoxia PET Tracers F-18 HX4, F-18 FAZA, and F-18 FMISO in a Preclinical Tumor Model, International Journal of Radiation Oncology Biology Physics, 91 (2015) 351–359.

[23]. Zhao D, Constantinescu A, Chang CH, Hahn EW, Mason RP, Correlation of tumor oxygen dynamics with radiation response of the dunning prostate R3327-HI tumor, Radiat Res, 159 (2003) 621–631. [PubMed: 12710873]

[24]. Diepart C, Karroum O, Magat J, Feron O, Verrax J, Calderon PB, Gregoire V, Leveque P, Stockis J, Dauguet N, Jordan BF, Gallez B, Arsenic trioxide treatment decreases the oxygen consumption rate of tumor cells and radiosensitizes solid tumors, Cancer Res, 72 (2012) 482–490. [PubMed: 22139377]

Author Manuscript Author Manuscript Author Manuscript Author Manuscript

[25]. Rodrigues LM, Howe FA, Griffiths JR, Robinson SP, Tumor R-2 * is a prognostic indicator of acute radiotherapeutic response in rodent tumors, Journal of Magnetic Resonance Imaging, 19 (2004) 482–488. [PubMed: 15065173]

[26]. Hallac RR, Zhou H, Pidikiti R, Song K, Stojadinovic S, Zhao D, Solberg T, Peschke P, Mason RP, Correlations of noninvasive BOLD and TOLD MRI with pO2and relevance to tumor radiation response, Magnetic Resonance in Medicine, 71 (2014) 1863–1873. [PubMed: 23813468]

[27]. Hallac RR, Zhou HL, Pidikiti R, Song K, Solberg T, Kodibagkar VD, Peschke P, Mason RP, A role for dynamic contrast-enhanced magnetic resonance imaging in predicting tumour radiation response, British Journal of Cancer, 114 (2016) 1206–1211. [PubMed: 27140315]

[28]. Ovrebo KM, Gulliksrud K, Mathiesen B, Rofstad EK, Assessment of tumor radioresponsiveness and metastatic potential by dynamic contrast-enhanced magnetic resonance imaging, Int J Radiat Oncol Biol Phys, 81 (2011) 255–261. [PubMed: 21816291]

[29]. Cao-Pham TT, Tran LB, Colliez F, Joudiou N, El Bachiri S, Gregoire V, Leveque P, Gallez B, Jordan BF, Monitoring Tumor Response to Carbogen Breathing by Oxygen-Sensitive Magnetic Resonance Parameters to Predict the Outcome of Radiation Therapy: A Preclinical Study, Int J Radiat Oncol Biol Phys, 96 (2016) 149–160. [PubMed: 27511852]

[30]. Zhao D, Jiang L, Hahn EW, Mason RP, Comparison of 1H blood oxygen level-dependent (BOLD) and 19F MRI to investigate tumor oxygenation, Magn. Reson. Med, 62 (2009) 357–364. [PubMed: 19526495]

[31]. Baudelet C, Gallez B, Current issues in the utility of blood oxygen level dependent MRI for the assessment of modulations in tumor oxygenation, Curr. Med. Imaging Rev, 1 (2005) 229–243.

[32]. Al-Hallaq HA, River JN, Zamora M, Oikawa H, Karczmar GS, Correlation of magnetic resonance and oxygen microelectrode measurements of carbogen-induced changes in tumor oxygenation, Int J Radiat Oncol Biol Phys, 41 (1998) 151–159. [PubMed: 9588930]

[33]. Matsumoto K, Bernardo M, Subramanian S, Choyke P, Mitchell JB, Krishna MC, Lizak MJ, MR assessment of changes of tumor in response to hyperbaric oxygen treatment, Magn Reson Med, 56 (2006) 240–246. [PubMed: 16795082]

[34]. Beeman SC, Shui YB, Perez-Torres CJ, Engelbach JA, Ackerman JJ, Garbow JR, O2 -sensitive MRI distinguishes brain tumor versus radiation necrosis in murine models, Magn Reson Med, 75 (2016) 2442–2447. [PubMed: 26175346]

[35]. White DA, Zhang Z, Li L, Gerberich J, Stojadinovic S, Peschke P, Mason RP, Developing oxygen-enhanced magnetic resonance imaging as a prognostic biomarker of radiation response, Cancer Lett, 380 (2016) 69–77. [PubMed: 27267808]

[36]. Arias-Ramos N, Pacheco-Torres J, López-Larrubia P, Magnetic Resonance Imaging Approaches for Predicting the Response to Hyperoxic Radiotherapy in Glioma-Bearing Rats., OBM Neurobiology, 3 (2019) 18.

[37]. Peschke P, Hahn EW, Wenz F, Lohr F, Braunschweig F, Wolber G, Zuna I, Wannenmacher M, Differential Sensitivity of Three Sublines of the Rat Dunning Prostate Tumor System R3327 to Radiation and/or Local Tumor Hyperthermia, Radiat. Res, 150 (1998) 423–430. [PubMed: 9768856]

[38]. Isaacs J, Heston W, Weissman R, Coffey D, Animal models of the hormone sensitive and insensitive prostatic adenocarcinomas, Dunning R3327-H, -HI and AT, Cancer Res, 38 (1978) 4353–4359. [PubMed: 698976]

[39]. Yang DM, Arai TJ, Campbell JW 3rd, Gerberich JL, Zhou H, Mason RP, Oxygen-sensitive MRI assessment of tumor response to hypoxic gas breathing challenge, NMR Biomed, 32 (2019) e4101. [PubMed: 31062902]

[40]. Pidikiti R, Stojadinovic S, Speiser M, Song KH, Hager F, Saha D, Solberg TD, Dosimetric characterization of an image-guided stereotactic small animal irradiator, Phys Med Biol, 56 (2011) 2585–2599. [PubMed: 21444969]

[41]. Karger CP, Peschke P, Scholz M, Huber PE, Debus J, Relative biological effectiveness of carbon ions in a rat prostate carcinoma in vivo: comparison of 1, 2, and 6 fractions, Int J Radiat Oncol Biol Phys, 86 (2013) 450–455. [PubMed: 23474116]

Author Manuscript Author Manuscript Author Manuscript Author Manuscript

[42]. Glowa C, Karger CP, Brons S, Zhao D, Mason RP, Huber PE, Debus J, Peschke P, Carbon ion radiotherapy decreases the impact of tumor heterogeneity on radiation response in experimental prostate tumors, Cancer Lett, 378 (2016) 97–103. [PubMed: 27224892]

[43]. Bourke VA, Zhao D, Gilio J, Chang CH, Jiang L, Hahn EW, Mason RP, Correlation of radiation response with tumor oxygenation in the Dunning prostate R3327-AT1 tumor, Int J Radiat Oncol Biol Phys, 67 (2007) 1179–1186. [PubMed: 17336219]

[44]. Kim DWN, Straka C, Cho LC, Timmerman RD, Stereotactic Body Radiation Therapy for Prostate Cancer: Review of Experience of a Multicenter Phase I/II Dose-Escalation Study, Frontiers in oncology, 4 (2014) 319–319. [PubMed: 25505731]

[45]. Zhao D, Pacheco-Torres J, Hallac RR, White D, Peschke P, Cerdan S, Mason RP, Dynamic oxygen challenge evaluated by NMR T1 and T2*--insights into tumor oxygenation, NMR Biomed, 28 (2015) 937–947. [PubMed: 26058575]

[46]. Little RA, Jamin Y, Boult JKR, Naish JH, Watson Y, Cheung S, Holliday KF, Lu H, McHugh DJ, Irlam J, West CML, Betts GN, Ashton G, Reynolds AR, Maddineni S, Clarke NW, Parker GJM, Waterton JC, Robinson SP, O'Connor JPB, Mapping Hypoxia in Renal Carcinoma with Oxygen-enhanced MRI: Comparison with Intrinsic Susceptibility MRI and Pathology, Radiology, 288 (2018) 739–747. [PubMed: 29869970]

[47]. Alonzi R, Padhani AR, Taylor NJ, Collins DJ, D'Arcy JA, Stirling JJ, Saunders MI, Hoskin PJ, Antivascular Effects of Neoadjuvant Androgen Deprivation for Prostate Cancer: An in Vivo Human Study Using Susceptibility and Relaxivity Dynamic Mri, International Journal of Radiation Oncology Biology Physics, 80 (2011) 721–727.

[48]. Zhou H, Hallac RR, Yuan Q, Ding Y, Zhang Z, Xie XJ, Francis F, Roehrborn CG, Sims RD, Costa DN, Raj GV, Mason RP, Incorporating Oxygen-Enhanced MRI into Multi-Parametric Assessment of Human Prostate Cancer, Diagnostics (Basel), 7 (2017) 48.

[49]. Chiu TD, Arai TJ, Campbell Iii J, Jiang SB, Mason RP, Stojadinovic S, MR-CBCT image-guided system for radiotherapy of orthotopic rat prostate tumors, PLoS One, 13 (2018) e0198065. [PubMed: 29847586]

[50]. Kerkmeijer LGW, Groen VH, Pos FJ, Haustermans K, Monninkhof EM, Smeenk RJ, Kunze-Busch M, Boer J.C.J.d., Zijp J.v.d.V.v., Vulpen M.v., Draulans C, Bergh L.v.d., Isebaert S, Heide U.A.v.d., Focal Boost to the Intraprostatic Tumor in External Beam Radiotherapy for Patients With Localized Prostate Cancer: Results From the FLAME Randomized Phase III Trial, Journal of Clinical Oncology, 0 JCO.20.02873.

[51]. Zheng X, Cui L, Chen M, Soto LA, Graves EE, Rao J, A Near-Infrared Phosphorescent Nanoprobe Enables Quantitative, Longitudinal Imaging of Tumor Hypoxia Dynamics during Radiotherapy, Cancer research, 79 (2019) 4787–4797. [PubMed: 31311808]

[52]. Peeters SG, Zegers CM, Lieuwes NG, van Elmpt W, Eriksson J, van Dongen GA, Dubois L, Lambin P, A comparative study of the hypoxia PET tracers [(1)(8)F]HX4, [(1)(8)F]FAZA, and [(1)(8)F]FMISO in a preclinical tumor model, Int J Radiat Oncol Biol Phys, 91 (2015) 351–359. [PubMed: 25491505]

[53]. Kelada OJ, Decker RH, Nath SK, Johung KL, Zheng M-Q, Huang Y, Gallezot J-D, Liu C, Carson RE, Oelfke U, Carlson DJ, High Single Doses of Radiation May Induce Elevated Levels of Hypoxia in Early-Stage Non-Small Cell Lung Cancer Tumors, International Journal of Radiation Oncology*Biology*Physics, 102 (2018) 174–183.

[54]. Rischin D, Hicks RJ, Fisher R, Binns D, Corry J, Porceddu S, Peters LJ, Trans-Tasman S Radiation Oncology Group, Prognostic significance of [18F]-misonidazole positron emission tomography-detected tumor hypoxia in patients with advanced head and neck cancer randomly assigned to chemoradiation with or without tirapazamine: a substudy of Trans-Tasman Radiation Oncology Group Study 98.02, J Clin Oncol, 24 (2006) 2098–2104. [PubMed: 16648512]

[55]. Lee N, Schoder H, Beattie B, Lanning R, Riaz N, McBride S, Katabi N, Li D, Yarusi B, Chan S, Mitrani L, Zhang Z, Pfister DG, Sherman E, Baxi S, Boyle J, Morris LGT, Ganly I, Wong R, Humm J, Strategy of Using Intratreatment Hypoxia Imaging to Selectively and Safely Guide Radiation Dose De-escalation Concurrent With Chemotherapy for Locoregionally Advanced Human Papillomavirus–Related Oropharyngeal Carcinoma, International Journal of Radiation Oncology Biology Physics, 96 (2016) 9–17.

Author Manuscript Author Manuscript Author Manuscript Author Manuscript

[56]. Zhou HL, Chiguru S, Hallac RR, Yang DH, Hao GY, Peschke P, Mason RP, Examining correlations of oxygen sensitive MRI (BOLD/TOLD) with F-18 FMISO PET in rat prostate tumors, American Journal of Nuclear Medicine and Molecular Imaging, 9 (2019) 156–+. [PubMed: 31139498]

[57]. Dewhirst MW, Birer SR, Oxygen-Enhanced MRI Is a Major Advance in Tumor Hypoxia Imaging, Cancer Res, 76 (2016) 769–772. [PubMed: 26837768]

Author Manuscript Author Manuscript Author Manuscript Author Manuscript

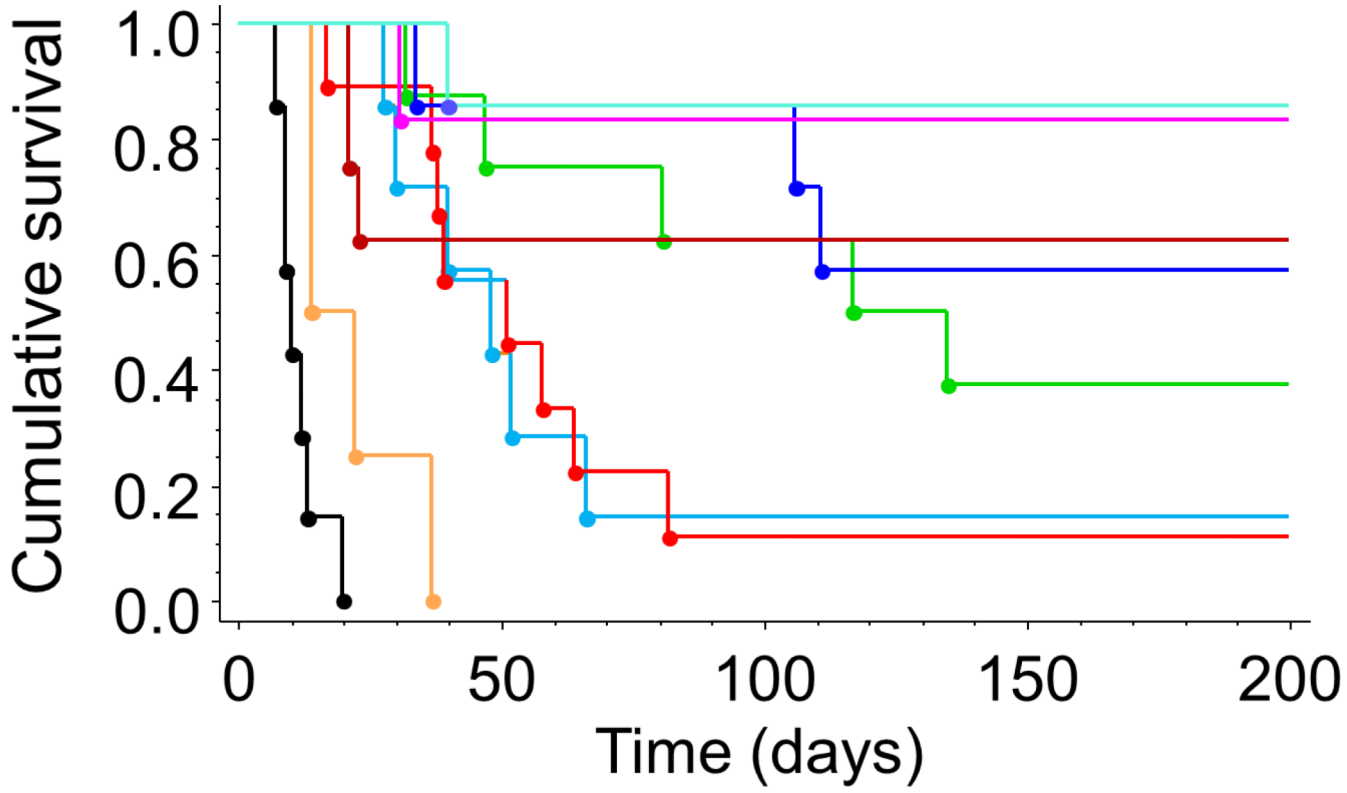

Figure 1. Radiation dose dependent tumor growth delay.

For rats breathing air during focal irradiation of AT1 tumors, Kaplan Meier plots show that higher radiation dose extended tumor growth delay and provided significantly better tumor control ($p<0.0001$). Below 30 Gy, there was no tumor control and above 80 Gy there was no obvious additional benefit. Black control; orange 10–20 Gy; light blue 30 Gy; red 40 Gy; green 50 Gy; dark blue 60 Gy; brown 70 Gy, pink 80 Gy; cyan 90 Gy.

Author Manuscript Author Manuscript Author Manuscript Author Manuscript

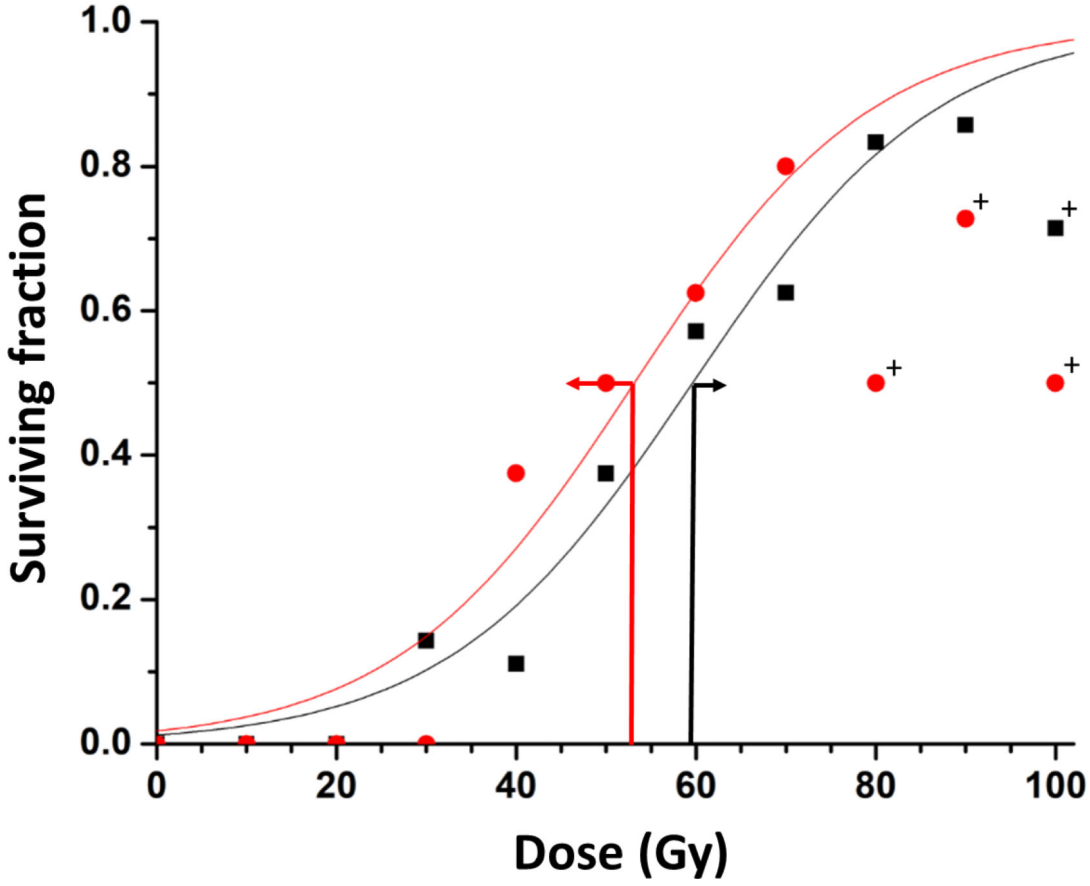

Figure 2. Dose Response Curves with respect to inhaled gas.

Data points represent the fraction of surviving rats at 200 days post irradiation. Separate curves are shown for tumors on rats breathing oxygen (red) or air (black) during focal irradiation. A distinct left shift is observed with TCD_{50} value decreasing from 59.6±1.5 to 53.1±3.1 Gy. Tumors on air breathing rats received doses of 0 (n=7), 10 (n=3), 20 (n-1), 30 (n=7), 40 (n=9), 50 (n=8), 60 (n=7), 70 (n=8), 80 (n=6), and 90 Gy (n=7) 100 (n=7) Gy and oxygen breathing rats received 10 (n=2), 20 (n=3), 30 (n=7), 40 (n=8), 50 (n=8), 60 (n=8), 70 (n=10), 80 (n=8), and 90 Gy (n=11), 100 Gy (n=10) respectively. Data are presented for all groups of tumors, but curves were locked to 0 and 120 Gy and data for doses >70 Gy excluded from fit for oxygen group and >90 Gy for air. Outliers (+) lie beyond 95% confidence intervals of fits. 95% error bars are shown at the estimated TCD_{50} (red and black arrows).

Author Manuscript Author Manuscript Author Manuscript Author Manuscript

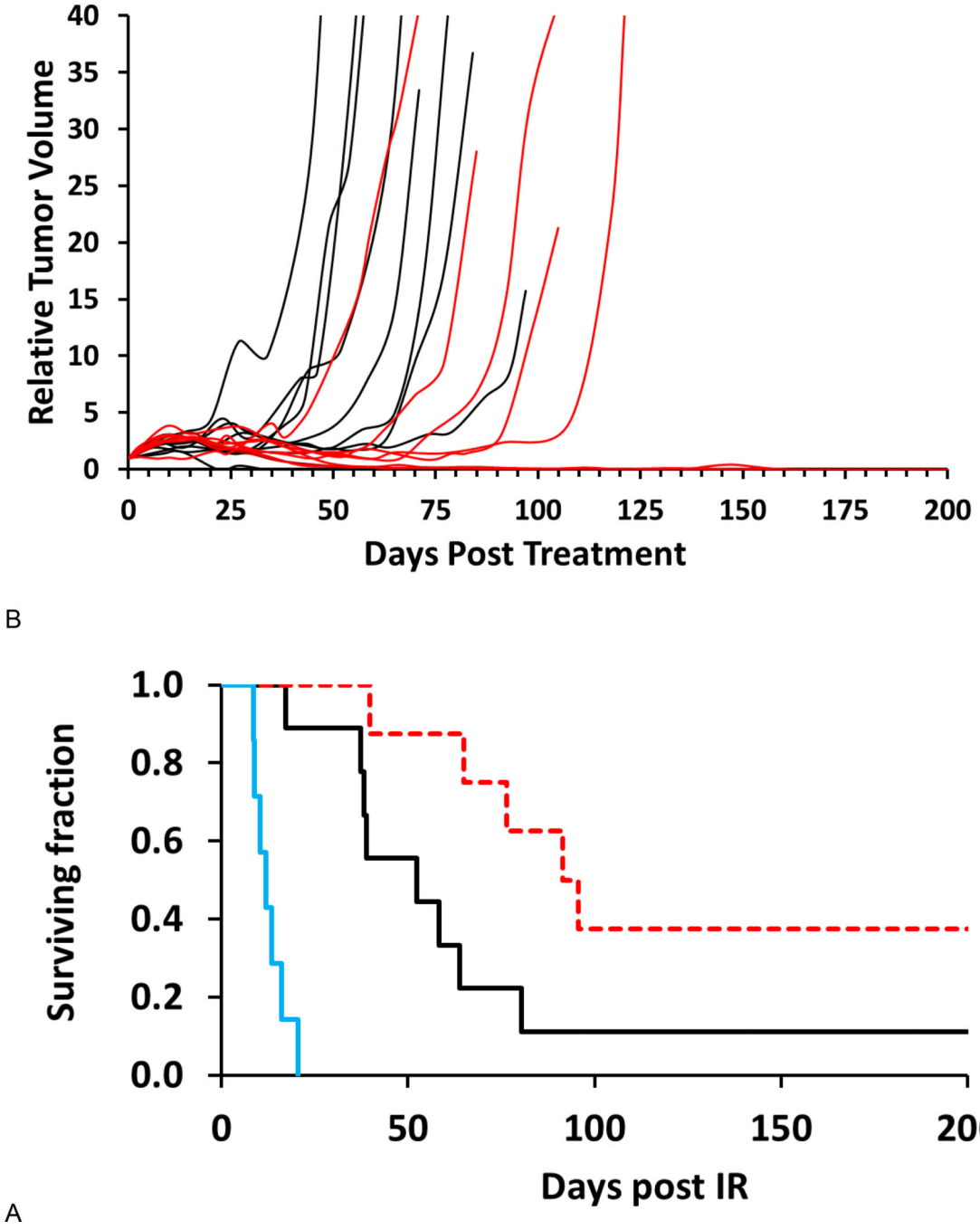

Figure 3. Influence of oxygen-breathing on tumor growth delay

A) Kaplan Meier plots of the surviving fractions with respect to inhaled gas. Unirradiated tumors (blue) had a volume quadrupling time (VQT) = 11 days. A dose of 40 Gy caused significant tumor growth delay for air breathing rats (black; VQT = 48 days; p=0.0002) with about 10% of tumors controlled at 200 days. When 40 Gy irradiation was accompanied with oxygen breathing (red), the growth delay was increased further: VQT = 74 days for tumors, which progressed, while 3 of 8 showed control; p=0.0201 *vs.* air and p=0.0002 *vs.* unirradiated).

Author Manuscript Author Manuscript Author Manuscript Author Manuscript

B) Growth curves for subcutaneous AT1 tumors following focal irradiation with 40 Gy when rats breathed either oxygen or air. Oxygen breathing (red) generally enhanced the tumor growth delay compared to the air-breathing animals (black), but there was obvious overlap. Most tumors continued to grow for about 10 days following irradiation before shrinking.

Author Manuscript Author Manuscript Author Manuscript Author Manuscript

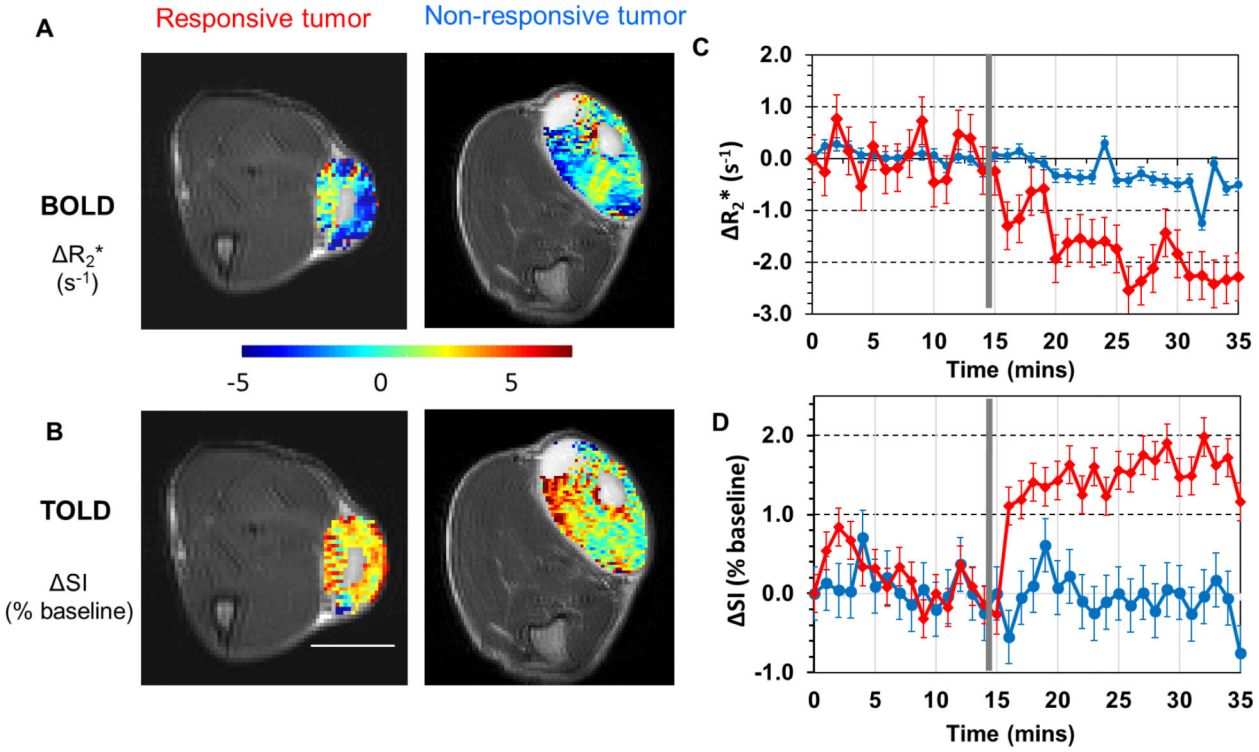

Figure 4. MRI and response to oxygen breathing challenge.

BOLD and TOLD maps overlaid on transaxial MR images from two representative R3327-AT1 tumors growing subcutaneously in the thigh of rats. A: ΔR_2* map (challenge - baseline) from BOLD measurements in a responsive and non-responsive tumor. B: corresponding T_1-weighted ΔSI map (challenge – baseline; expressed as % of baseline SI) maps from TOLD measurements. White bar represents 1 cm. C and D) Traces show BOLD (mean quantitative ΔR_2* with baseline standard deviations) and TOLD (mean semi-quantitative T_1-weighted signal intensity with baseline standard deviations) responses to oxygen gas breathing challenge for the responsive (red) and unresponsive (blue) tumors presented in A and B. The vertical grey line indicates transition from air to oxygen breathing.

Author Manuscript Author Manuscript Author Manuscript Author Manuscript

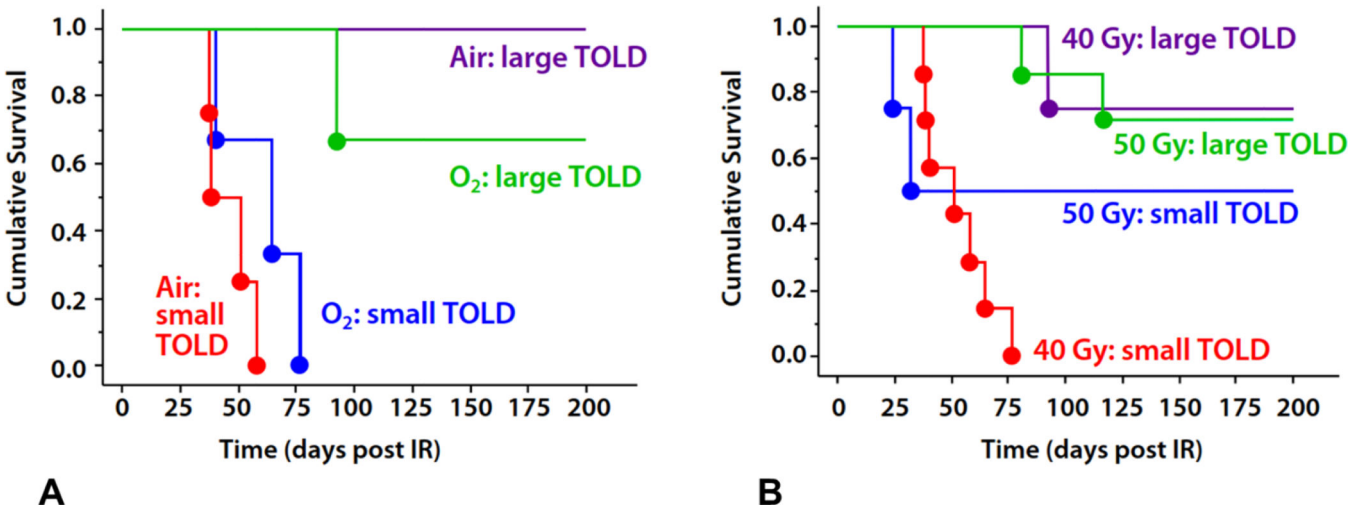

Figure 5. Kaplan Meier plots stratified by TOLD MRI.

A) Tumors exhibiting small TOLD response (<0.922%ΔSI) showed poor tumor control following a single dose of 40 Gy whether the rats breathed air (red, n=4) or oxygen during irradiation (blue, n=3). Meanwhile, those tumors exhibiting a large TOLD response showed effective control irrespective of inhaled gas (green and purple, n=3 and 1 and respectively) B) Noting the similarity of response irrespective of inhaled gas, we combined groups in (A) to show curves for mixed cohorts, which include both air and oxygen, gas breathing rats. It is seen that tumors showing a small TOLD MRI response to pre-irradiation oxygen breathing challenge were not controlled whether breathing air or oxygen during irradiation (red). Applying a higher radiation dose (50 Gy) to tumors showing small TOLD response improved tumor control in 50% of tumors (blue). Well oxygenated tumors, characterized by a large TOLD response showed similar control with 40 or 50 Gy irrespective of inhaled gas (purple and green).

Author Manuscript Author Manuscript Author Manuscript Author Manuscript

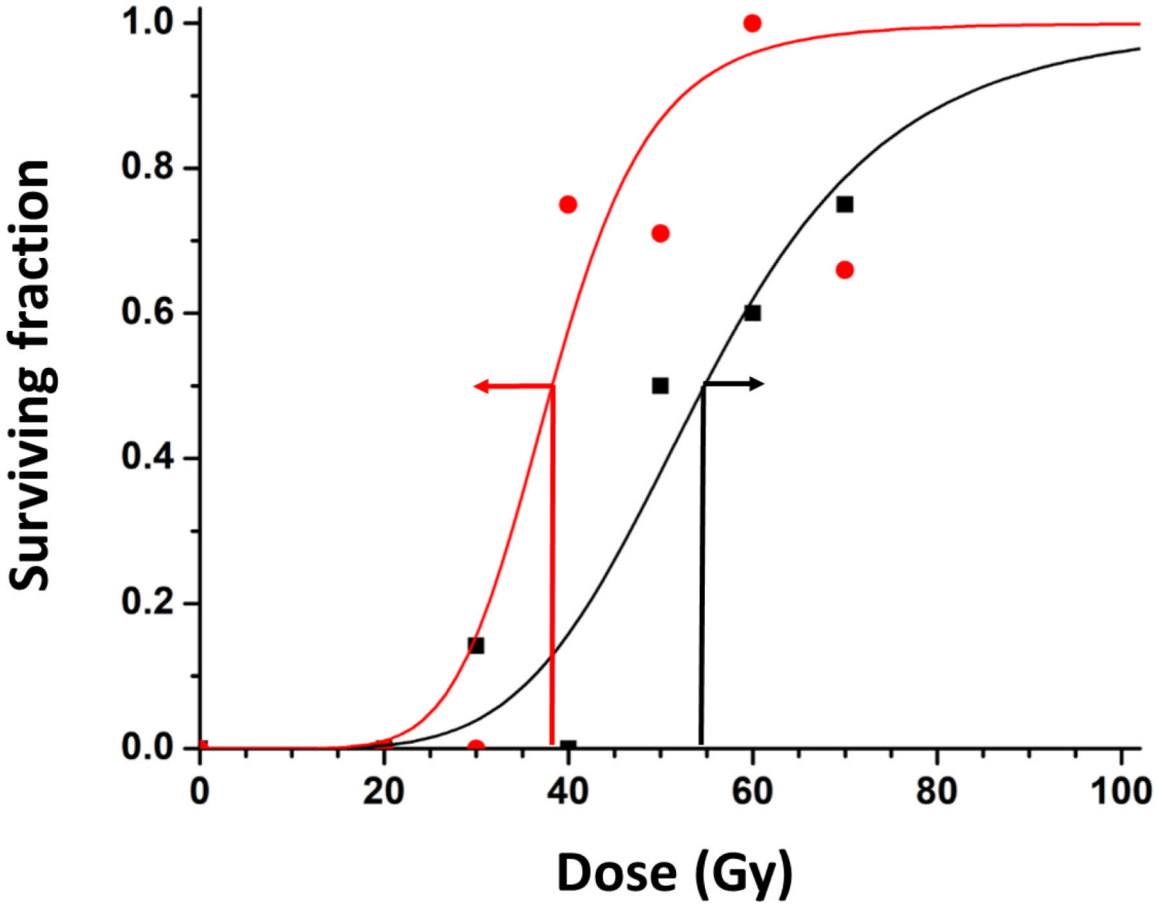

Figure 6. Dose Response Curves with respect to inhaled gas.

Survival curves are shown for groups of tumors irradiated while rats breathed air or oxygen with stratification based on TOLD signal response to an oxygen gas breathing challenge before irradiation: T_1W ΔSI> 0.922% (red) or <0.922% (black), yielding distinctly separate curves with TCD_{50} 36.2±3.2 versus 54.7±2.4 Gy. 95% error bars are shown at the estimated TCD_{50} (red and black arrows).